



1 **Phytoplankton growth and physiological responses to a plume front in the 2 northern South China Sea**

3 Qian P. Li ^{1,2,*}, Weiwen Zhou ^{1,2}, Yinchao Chen ^{1,2}, and Zhengchao Wu¹

4 ¹South China Sea Institute of Oceanology, Chinese Academy of Sciences, Guangzhou 510301, China

5 ²University of Chinese Academy of Sciences, Beijing 100049, China

6 *Corresponding to:* Qian Li (qianli@scsio.ac.cn)

7

8 **Abstract.** Due to a strong river discharge during April-June 2016, a persistent salinity front, with
9 freshwater flushing seaward on the surface but seawater moving landward at the bottom, was formed in
10 the coastal waters west of the Pearl River Estuary (PRE) over the Northern South China Sea (NSCS)
11 shelf. Hydrographic measurements revealed that the salinity front was influenced by both river plume
12 and coastal upwelling. Shipboard nutrient-enrichment experiments with size-fractionation chlorophyll-*a*
13 measurements were performed on both sides of the front as well as the front zone to diagnose the spatial
14 variations of phytoplankton physiology across the frontal system. We also assessed the size-fractionated
15 responses of phytoplankton to the treatment of plume water at the frontal zone and the seaside of the
16 front. Biological impact of vertical mixing or upwelling was further examined by the response of
17 surface phytoplankton to the addition of local bottom water. Our results suggested that there was a large
18 variation of phytoplankton physiology on the seaside of the front driven by dynamic nutrient fluxes,
19 although P-limitation was prevailing on the shore-side of the front and at the frontal zone. The
20 spreading of plume water at the frontal zone would directly improve the growth of micro-phytoplankton,
21 while nano- and pico-phytoplankton growths could become saturated at high percentages of plume
22 water. Also, the mixing of bottom water would stimulate the growth of surface phytoplankton on both
23 sides of the front by altering the surface N/P ratio closer to the Redfield stoichiometry. In summary,
24 phytoplankton growth and physiology could be profoundly influenced by physical dynamics of the
25 frontal system during the spring-summer of 2016.



1 **1 Introduction**

2 It is well known that physical dynamics of coastal ocean can be strongly influenced by river input.
3 When there is a high river discharge, a large plume of brackish water can form near the estuary mouth
4 and the adjacent inner shelf regions, which is generally a low-salinity mesoscale feature that disperses
5 fresh river water across the coastal margin (Horner-Devine et al., 2015). River plumes can transport and
6 redistribute river-borne materials, such as nutrients and particles, and thus largely affect
7 biogeochemistry of the coastal ocean (Dagg et al., 2004; Lohrenz et al., 2008). Convergent surface
8 fronts over the shelf are a common feature associated with river plumes (e.g. Garvine and Monk, 1974).
9 These plume-induced fronts are often the places of high phytoplankton productivities (Acha et al., 2004)
10 and thus provide important feeding and reproductive habitats for higher trophic-level marine organisms,
11 such as zooplankton and fish (Morgan et al., 2005).

12 Biological production of the coastal Northern South China Sea (NSCS) is controlled by
13 monsoon-driven upwelling that brings nutrient-rich deep waters to the shelf (Liu et al., 2002). In
14 addition, there is an intense river discharge from the Pearl River Estuary (PRE) during the
15 spring-summer leading to the development of a strong river plume nearshore (Su, 2004). In the coastal
16 water west of the PRE, convergence between the northeastward coastal current and the southeastward
17 river plume can maintain a sharp salinity front along the shelf when the southwest monsoon is
18 prevailing over the region (Wong et al., 2003). Variability of the front is primarily controlled by the
19 river discharge and by the direction and magnitude of the regional wind field (Dong et al., 2004). On the
20 east of the PRE, the surface plume water can be entrained in the coastal current as a salinity tongue in
21 the summer and propelled eastward and offshore by wind-driven jets to affect the large area of the
22 NSCS shelf-sea (Gan et al., 2009).

23 The plume front over the NSCS shelf creates an interface between the river plume and the adjacent
24 marine waters with rapid changes of both salinity and nutrients at the frontal zone (e.g. Cai et al., 2004).
25 There is a P-limitation of phytoplankton in the river plume due to a high N/P ratio of the PRE water
26 (Zhang et al., 1999; Yin et al., 2001). In contrast, biological production is generally N-limited in the
27 offshore oceanic waters (Wu et al., 2003; Chen et al., 2004), as the upwelled deep-water with an N/P



1 ratio of ~14 is essentially N-deficient compared to the Redfield N/P ratio of 16 (Wong et al., 2007). A
2 shift from P-limitation to N-limitation of phytoplankton community across the plume edge to the sea
3 has been speculated based on results of the Hong Kong waters (Yin et al., 2001). Results of a
4 physical-biogeochemical coupling model in the NSCS indeed predict a fast decrease of N/P ratio from
5 ~120 in the near-field to <13.3 in the far-field of the plume front driven by a higher N/P consumption
6 ratio and by mixing with the ambient lower N/P water (Gan et al., 2014).

7 Nutrient variations, in addition to light fluctuation, can affect the partitioning of phytoplankton
8 biomass between different size classes (Marañón et al., 2012, 2015). The change of phytoplankton size
9 structure can be controlled by size-dependent trade-off processes for resource acquisition and use
10 (Marañón, 2015). Small phytoplankton has a higher nutrient affinity for growth under nutrient limiting
11 conditions (Suttle, 1991; Raven et al., 1998), whereas large phytoplankton shows higher growth
12 efficiency under favorable nutrient conditions (Cermeño et al., 2005). A large shift of phytoplankton
13 assemblage from small to large cells could arise following the addition of nutrients from deep seawater
14 in the North Pacific Subtropical Gyre (McAndrew et al., 2007). The success of large phytoplankton in
15 the oligotrophic ocean would highly depend on external environmental dynamics, although it has the
16 metabolic potential of enhance production (Alexander et al., 2015). It is thus important to understand
17 not only the mechanisms for nutrient variations, but also the response of size-fractionated
18 phytoplankton community to the diverse nutrient supplies, particularly at the frontal zone where the
19 patchiness of phytoplankton can be affected by complex physical dynamics (Li et al., 2012).

20 Three field surveys were carried out to study the biological response to a strong salinity front over
21 the NSCS shelf during the April-June of 2016. Besides comprehensive hydrographic and
22 biogeochemical measurements, such as temperature, salinity, nutrients, and chlorophyll-*a*, we
23 performed nutrient-enrichment experiments with size-fractionation chlorophyll-*a* measurements at the
24 shore-side, the frontal zone, and the seaside of the front to examine the spatial change of phytoplankton
25 physiology. Phytoplankton response to the river plume at the frontal zone was addressed by mixing the
26 local surface water with a varying percentage of plume water from the shore-side of the front. The
27 impact of river plume on the seaside of the front was further examined by incubations of the surface



1 seawater with the treatment of plume water. In addition to these experiments, the bottom water was
2 added to the surface water for incubation at various zones of the frontal system to estimate the impact of
3 vertical mixing or upwelling on surface phytoplankton community. We hope to use these experimental
4 approaches to address the responses of phytoplankton growth and physiology to the strong salinity front
5 over the shelf. Based on these field results, we will also discuss the impacts of river plume, vertical
6 mixing and coastal upwelling on physical and biogeochemical dynamics of the frontal systems in the
7 NSCS shelf-sea.

8

9 **2. Material and methods**

10 **2.1 Description of the field work**

11 Three field cruises aboard *R/V Zhanjiang Kediao* were performed during April, May, and June in 2016
12 with hydrographic and biogeochemical samplings over the NSCS shelf (Fig.1). A vertical transect
13 across the salinity front from the inner estuary to the shelf was intensively sampled during the June
14 (Section A in Fig. 1). There were three other transects (Section B, C, and D in Fig. 1) outside the PRE
15 with intense size-fractionation chlorophyll-*a* measurements during both May and June. Section B
16 transited across the frontal zone with Sections C and D on the seaside of the front. Surface waters at
17 different zones of the salinity front were selected for nutrient-enrichment experiments, including the
18 shore-side of the front (S1 and S2), the frontal zone (S3 and S4), and the seaside of the front (S5, S6 and
19 S7) during May and June 2016.

20

21 **2.2 Measurements of hydrography, chlorophyll-*a*, nutrients and phytoplankton size structure**

22 Seawater temperature, salinity, pressure, and fluorescence were acquired using a SeaBird model
23 SBE9/11 conductivity-temperature-depth (CTD) recorder and a Chelsea Aqua fluorometer. Discrete
24 water samples at 1m, 20m, 40m, 60m, 80m, and 100m were collected with Niskin bottles mounted onto
25 a Rosette sampling assembly (General Oceanic). After filtration onto a Whatman GF/F glass fiber filter,
26 the chlorophyll-*a* (Chl-*a*) sample was extracted by 90% acetone in darkness at 4 °C for 24 h and



1 determined using a Turner Design fluorometer (Knap et al., 1996). Three types of filters (20 μm Nylon
2 filter, 2 μm Polycarbonate filter, and 0.7 μm GF/F filter) were used to produce three different
3 size-classes including micro- ($>20\ \mu\text{m}$), nano- (2-20 μm), and pico-phytoplankton (0.7-2 μm). Nutrient
4 samples were collected inline through a Whatman GF/F filter and frozen immediately at -20 $^{\circ}\text{C}$ until
5 analyzed. After thawing at room temperature, they were analyzed by an AA3 nutrient auto-analyzer
6 using colorimetric methods (Knap et al., 1996) with detection limits of 0.02, 0.02, and 0.03 $\mu\text{mol L}^{-1}$,
7 for nitrate plus nitrite (N+N), soluble reactive phosphate (SRP), and silicate (Si), respectively.

8

9 **2.3 Setup of the ship-board incubation experiments**

10 There were four different treatments prepared in duplicate for nutrient-enrichment experiments
11 including the control (C), nitrogen alone (+N), phosphorus alone (+P), and nitrogen plus phosphorus
12 (+NP). Nutrients were added to the incubation bottle to obtain final concentrations of 4.8 μM NaNO_3
13 and 0.3 μM NaH_2PO_4 . Seawater samples were prescreened through a 200 μm mesh to remove large
14 grazers. These samples were incubated in 2.4 L transparent acid-cleaned polycarbonate bottles and
15 placed in a shipboard incubation chamber equipped with a flow-through seawater system. The incubator
16 was shaded to mimic 30% sunlight using a black filter with each bottle manually stirred twice a day.
17 Each incubation experiment lasted for two days with size-fractionated chlorophyll-*a* samples taken once
18 a day.

19 Surface water (~50L) collected at S2 outside the PRE mouth was saved as the plume water (PW).
20 Half of the PW was filtered through a 0.2 μm Millipore membrane filter (GTTP IsoporeTM) to produce
21 the filtered plume water (FPW). These waters were used to dilute the local surface waters at S6, S7 and
22 S8. Under the in-situ temperature and light, the mixture was incubated on board for two days with
23 size-fractionation chlorophyll-*a* collected each day. The bottom waters (BW) were collected at S2, S4,
24 S6 and S7 and stored in clean HDPE carboy. A 0.2- μm -filtration was used to create the filtered bottom
25 water (FBW). Both BW and FBW, with a final percentage of 12.5%, were added to the local surface
26 water for incubation to study the biological impact of vertical mixing or upwelling at these stations. We
27 also conducted a series of mixing experiments between surface waters of S2 and S4 with the final



1 percentages of 0%, 25%, 50%, 75%, and 100% for S2, corresponding to the final salinity of 30.7, 24.7,
2 18.7, 12.7, and 6.6, respectively.

3 For each size class, the rate of daily chlorophyll-*a* production ($\mu\text{g L}^{-1} \text{d}^{-1}$) was calculated by the
4 difference of size-fractionated chlorophyll-*a* concentration during each incubation day. We also
5 estimated the net growth rates μ (d^{-1}) for the water mixing experiment between S2 and S4 by μ
6 $=\ln(Chl_1/Chl_0)/\Delta t$, with Chl_0 and Chl_1 the initial and final size-fractionated chlorophyll-*a* concentrations
7 every day ($\Delta t = 1$ day). The specific growth rate approach could not work for other experiments, as large
8 errors of μ would arise when the initial chlorophyll-*a* of a certain size-class (Chl_0) was close to zero.

9

10 **2.4 Estimations of horizontal advection and vertical mixing at the seaside of the front**

11 Assuming a salinity balance at the seaward front (Fong and Geyer, 2001), we have

12
$$U_e(S_0 - S) = K_H \frac{\partial S}{\partial z} \quad (1)$$

13 where S and S_0 are salinity of the plume front and ambient water, K_H is the eddy diffusivity, and the
14 bulk entrainment rate U_e is computed by $U_e \approx 0.038Ri^{-0.5}(\tau/\rho)^{0.5}$ with the Richardson number (Ri) given
15 by

16
$$Ri = \frac{g\rho}{\tau\rho_0} \int_0^h (\rho_0 - \rho) dz \quad (2)$$

17 with g the gravitational acceleration, ρ_0 the ambient density, h the thickness of plume front and τ the
18 wind stress (Fong and Geyer, 2001).

19 Horizontal nitrate flux to the surface water on the seaside of the front can thus be estimated by J_h
20 $= U_e(N - N_0)$ with N and N_0 the nutrient concentrations of the plume front and the ambient water. The
21 vertical nitrate flux can be estimated by $J_v = K_H(\partial N / \partial z)$.

22



1 **3 Results**

2 **3.1 Physical and biogeochemical setting of the NSCS shelf during the spring-summer**

3 The temperature versus salinity diagram revealed a large change of hydrography during the three
4 cruises (Fig. 2). There was a regional warming effect over shelf from April to June (Fig. 3A1-A3),
5 along with the increase of wind strength (with a regional shift to upwelling favorable wind after the
6 May, data no shown). The riverine input was clearly evidenced with low salinity waters in all the three
7 cruises (Fig. 2). Spatially, there was a large area of low salinity in the coastal water west of the PRE
8 (Fig. 3B1-B3), leading to a strong salinity front in the inner shelf. The plume water was mostly on the
9 shore side of the front when the river-outflow flowing westward along the shore. The shore-side of the
10 front was defined by a salinity of <26, the nearshore boundary of the plume (Wong et al., 2003), with
11 the seaside of the front by a salinity of >32, the offshore boundary of the plume (Ou et al., 2007). The
12 frontal zone is thus located in between the nearshore and offshore boundaries of river plume (Fig. 1).

13 In the coastal water west of the PRE, there was an intense chlorophyll-*a* bloom (Chl-*a* > 5 µg/L)
14 on the shore-side of the front during all the three cruises (Fig. 3C1-C3), although the surface
15 temperature of the bloom area increased from ~22 °C in April, to ~26 °C in May and to ~31 °C in June.
16 The surface distributions of nitrate, silicate, and phosphate generally follow that of salinity for all the
17 three cruises with much higher concentrations on the shore-side of the front than the seaside of the front
18 (Fig. 3D and 3F). Interestingly, the surface low salinity tongue in the coastal water east of the PRE by
19 eastward plume dispersion was cut off by a water mass of low temperature but high salinity during the
20 June (Fig. 3A3 and 3B3). This water presumably should come from the subsurface via coastal
21 upwelling, which was further supported by its higher phosphate concentration but lower N/P ratio
22 compared to the ambient waters (Fig. 3D3 and 3F3).

23 There were substantial vertical changes of temperature, salinity, and chlorophyll-*a* while crossing
24 the salinity front (Fig. 4A-4C) from the estuary to the shelf (Section A). The surface front was located
25 in the inner shelf with the subsurface frontal zone going deep to the bottom of the estuary mouth
26 (Fig. 4A). Vertical distributions of nutrients generally followed that of salinity in the PRE with higher
27 surface concentrations, whereas there was large drawdown of nutrients on the shore-side of the front



1 when approaching the edge of the river plume (Fig. 4D-4F), corresponding to a fast decrease of N/P
2 ratio from the shore-side of the front to the frontal zone. The dominant size-class shifted from micro- to
3 pico-cells while crossing the salinity front from the shore in Section B for both the May and June
4 cruises (Fig. 5). Variations in the percentages of micro- and nano-cells in Sections C and D were due to
5 a spatial change of the frontal zone (Fig. 5).

6

7 **3.2 Variations of phytoplankton nutrient limitation over the NSCS shelf**

8 Surface water properties of the incubation stations were summarized in Table 1. The highest
9 concentrations of nutrients and chlorophyll-*a* were in S1 and S2 on the shore-side of the front where
10 micro- and nano-cells dominated. A P-deficiency of the plume water can be inferred from the high N/P
11 ratios there. There was higher salinity (~30) but lower chlorophyll-*a* (~1 µg/L) in S3 and S4 at the
12 frontal zone, which should reflect a reduced impact of river plume. The surface waters of S5, S6 and S7
13 on the seaside of the front were dominated by pico-phytoplankton and showed the typical characteristics
14 of the open NSCS with low nutrients and chlorophyll-*a* but high salinity.

15 Phytoplankton total chlorophyll-*a* on the shore-side of the front (S1 and S2) and at the frontal zone
16 (S3 and S4) showed responses to P-addition but not N-addition, suggesting of P-limitation in these
17 waters (Fig. 6A-6D). In contrast, phytoplankton nutrient limitation varied substantially at S5, S6, and S7
18 on the seaside of the front (Fig. 6E-6G). Total chlorophyll showed no response to N-addition,
19 P-addition, and N-plus-P addition at S5 (Fig. 6E), which should suggest a relief of phytoplankton
20 community from N- and P-stresses there. There was a N-limitation of phytoplankton at S6, as the total
21 chlorophyll-*a* increasing with N-addition but not with P-addition (Fig. 6F), which was consistent with
22 its low N+N concentration of <0.5 µM at the surface (Table 1). Phytoplankton growth was P-limited at
23 S7 during the first day of incubation, but it became co-limited by both N and P during the second day of
24 incubation (Fig. 6G). This station (S7) was on the shelf edge, far away from the frontal zone, but was
25 influenced by the eastward extension of the plume as indicated by its relatively low surface salinity.

26 Interestingly, the response of phytoplankton total chlorophyll-*a* to nutrient treatments was mostly



1 mediated by micro-cells at stations S1, S2, and S3 where high nutrient concentrations and N/P ratios
2 were found (Fig. 6A2-6C2). In contrast, for stations S5, S6 and S7 on the seaside of the front, the
3 change of phytoplankton total chlorophyll-*a* at the surface layer was largely controlled by
4 pico-phytoplankton (Fig. 6D2-6G2). This result is consistent with the contention that larger
5 phytoplankton grow faster than small cell under nutrient replete conditions.

6

7 **3.3 Responses of surface phytoplankton to the addition of plume water**

8 The result of mixing experiments between the surface waters of S2 and S4 was shown in Fig. 7. The
9 total chlorophyll-*a* was proportional to the amount of PW (the surface water of S2) in the mixture (Fig.
10 7A). As the PW has more chlorophyll-*a* than S4 (Table 1), the initial chlorophyll-*a* concentration of the
11 mixture showed a linear increase with the percentage of PW. The three phytoplankton size-classes
12 showed distinct responses to the ascending PW percentage during the first day of incubation (Fig. 7B).
13 There was a linear increase of the daily chlorophyll-*a* production rate of micro-cells with the percentage
14 of PW ($r^2=0.9, p<0.01$), whereas the production rate of nano-cells first increased with the PW
15 percentage from 0% to 50% and then remained relatively stable from 50% to 100%. Apart from both
16 micro- and nano-cells, pico-phytoplankton reached the maximal production rate at the 50% of PW
17 treatment. The responses of net growth rates to various PW treatments were slightly different from
18 those of the chlorophyll-*a* production rates (Fig. 7C). The net growth rate of micro-phytoplankton
19 increased with the PW percentage before becoming saturated at 75-100% PW. Pico-phytoplankton
20 showed a higher net growth rate but lower daily chlorophyll-*a* production rate than nano-phytoplankton
21 during the first day of incubation in the cases of 50-100% PW treatments. As the nutrients running out,
22 there were decreases of net growth rates for all the size-classes during the second day of incubation.

23 The chlorophyll-*a* biomass, as well as the daily chlorophyll-*a* production rate, of phytoplankton
24 was substantially enhanced by the addition of FPW at S6, S7, and S8 (Fig. 8). This should be expected
25 as the plume water had much more nutrients than the local waters on the seaside of the front. The
26 response of phytoplankton community to FPW was largely determined by nano- and pico-cells at these
27 stations. At station S6, the raw plume water (PW) was also added to the surface water for incubation to



1 account for the advective chlorophyll input by the river plume. Although the amount of PW added was
2 only 12.5%, it contributed about half of the chlorophyll biomass to the mixture for S6, which was due to
3 the high chlorophyll-*a* concentration of PW. That is why a stronger response of phytoplankton
4 chlorophyll-*a* to PW than to FPW was observed (Fig. 8A).

5

6 **3.4 Responses of surface phytoplankton to the addition of bottom waters**

7 The addition of FBW increased the total chlorophyll-*a* of S2, which was largely contributed by
8 micro-cells (Fig. 9A). At this station, the inclusion of FBW (lower N/P ratio) reduced the N/P ratio of
9 the surface water and thus the P-stress of surface phytoplankton. We found no difference in chlorophyll
10 responses to FBW and BW at S2, which could be due to the low chlorophyll-*a* of BW. Interestingly,
11 there was a net loss of phytoplankton chlorophyll-*a* with time at S4, which was not affected by the FBW
12 treatment (Fig. 9B). This is because nitrate and phosphate concentrations of the surface water were
13 similar to those of the FBW, although there was 9-fold increase of silicate in the FBW (Table 1). The
14 elevated silicate after FBW treatment did not stimulate a diatom growth given the sparse of micro-cells
15 in the surface water there. The addition of BW, however, substantially decreased the total chlorophyll-*a*
16 (Fig. 9B), likely reflecting the grazing activity in BW.

17 Phytoplankton growth was promoted by the FBW addition at S6 (Fig. 9C), as the N-stress of
18 phytoplankton could be relieved by the FBW with higher nitrate concentration and N/P ratio. We found
19 a reduced phytoplankton growth with the addition of BW compared to that of FBW (Fig. 9C), which
20 could also be attributed to the grazing activity of BW. At station S7, the BW was from the depth of 109
21 m with high nutrients but negligible chlorophyll-*a* compared to the surface water (Table 1). Therefore,
22 both FBW and BW additions increased surface phytoplankton growth (Fig. 9D). This stimulating effect
23 could be attributed to a reduced P-stress of phytoplankton in response to a lower N/P ratio of the surface
24 water.

25

26 **4 Discussion**



1 The persistent salinity front we observed from April to May of 2016 was a plume-induced buoyant front
2 (e.g. Ou et al., 2007), which could appear when the freshwater discharge was much stronger than the
3 tidal effect (Garvine and Monk, 1974). While governed by buoyancy, planetary rotation, and wind
4 forcing (Wong et al., 2003), the impact of the plume front on the coastal NSCS was large, as the low
5 salinity water spreading westward and eastward onto the large area of the shelf. A chlorophyll bloom on
6 the shore-side of the front was a direct response of phytoplankton to the river plume (Harrison et al.,
7 2008), as nutrient replenishment from the subsurface could be restricted by the salinity front with a
8 persistent stratification at the frontal zone. On the other hand, there was an intense upwelling found near
9 the coastal water east of the PRE, which could be due to an intensified cross-isobath transport of the
10 bottom boundary layer driven by an amplified alongshore current (Gan et al., 2009). Therefore, the
11 frontal system was affected by both river plume and coastal upwelling during the spring-summer of
12 2016.

13 Phytoplankton growth over the shore-side of the front was essentially P-limited, which is
14 consistent with previous findings (Zhang et al., 1999; Yin et al., 2001). Phytoplankton P-stress here is a
15 physiological response to the P-deficiency of the river plume due to the stoichiometric lack of P relative
16 to N (Moore et al., 2013). However, we found a spatial difference of phytoplankton physiology on the
17 seaside of the front, where there was less influence of river plume from the perspective of salinity.
18 Phytoplankton growth over the seaside of the front, dominated by small pico-cells, could be P-limited,
19 or N-limited, or not limited by N and P. There was no evidence of Si-limitation since micro-cell was not
20 stimulated by the filtered bottom water with a much higher silicate concentration. The spatial difference
21 of phytoplankton physiology is consistent with the nutrient variation of the developing plume front,
22 which should be regulated by both biological uptake and physical dynamics (Gan et al., 2014).

23 A balance between horizontal advection and vertical mixing can be approximately maintained at
24 the seaward front by an Ekman straining mechanism (Fong and Geyer, 2001) with salinity gradients
25 created by cross-shore Ekman current but destroyed by vertical mixing. Based on the hydrographic data,
26 we can estimate a horizontal entrainment rate U_e of $0.5\text{--}1.0 \times 10^{-5}$ m/s and a vertical diffusivity K_H of
27 $0.8\text{--}1.7 \times 10^{-4}$ m²/s across frontal boundary, which are comparable to those previously found over the



1 NSCS shelf (St. Laurent, 2008; Li et al., 2016). Horizontal nitrate flux to the seaside of the front is thus
2 0.2-3.6 mmolN/m²/d. If we assume the same K_H for the seaside of the front, we can also roughly
3 estimate a vertical nitrate diffusive flux of 0.6-4.7 mmolN/m²/d, which is on the same order of
4 magnitude as the horizontal nutrient fluxes. Therefore, the varying nutrient supply driven by physical
5 dynamics, including cross-front advection and vertical mixing, might be responsible for the variability
6 of phytoplankton physiology on the seaside of the front.

7 The influence of river plume on the surface phytoplankton at the frontal zone was to directly
8 stimulate micro-phytoplankton growth, while a community P-limitation was still prevailing. Although
9 the growths of nano- and pico-cells were improved by low percentages of plume water (<50%), they
10 were inhibited by high percentages of plume water (>50%). This finding is consistent with the
11 different nutrient uptake kinetics of the three phytoplankton size-classes (Finkel et al., 2009).
12 Micro-phytoplankton generally has a larger half-saturation constant for nutrient uptake than nano- and
13 pico-phytoplankton (Cermenio et al., 2005; Litchman et al., 2007). Therefore, small phytoplankton
14 (nano- and pico-cells) could become saturated with the ascending nutrients before micro-phytoplankton
15 did. At the frontal zone, nano-phytoplankton growth even well exceeded micro-phytoplankton at a low
16 percentage of plume water (<50%), which could explain the enhanced biomass percentage of nano-cells
17 at the frontal zone. On the seaside of the front, the plume-water addition (12.5%) indeed improved the
18 growths of all the three phytoplankton size-classes, regardless the type of nutrient limitation the surface
19 phytoplankton originally experienced.

20 Different from the shore-side of the front with a sharp decrease of nutrients at depths, the bottom
21 water on the seaside of the front showed much higher nutrient concentrations (but lower N/P ratios)
22 than the surface water, which was due to the intrusion of the deep water (Gan et al., 2014). Thus,
23 surface nutrient concentrations after vertical mixing or upwelling should decrease on the shore-side of
24 the front but increase on the seaside of the front. The final consequence of vertical mixing on both sides
25 of the front was to alter the N/P ratio of surface water closer to the Redfield ratio of 16 and thus
26 improved the growth of phytoplankton as showed in our experiments. While microplankton growth was
27 slightly stimulated by BW addition, our results on the seaside of the front did not show a shift of



1 phytoplankton community from pico- to micro-cells in response to upwelled nutrients from
2 deep-water-additions found in the western South China Sea (Cui et al., 2016) and in the open ocean
3 (McAndrew et al., 2007). In addition to nutrient stresses by varying nutrient concentrations and ratios,
4 phytoplankton growth at the frontal zone should also be influenced by other factors such as the change
5 of grazing pressure (Li et al., 2012). There were indeed evidences of enhanced grazing activity at
6 stations S4 and S6 when comparing incubation results of the filtered bottom water with those without
7 filtration. Therefore, a further study of grazing impact of zooplankton on various sizes of phytoplankton
8 and subsequent biomass accumulation at the frontal zone of the NSCS shelf may be a future research
9 priority. Since we have only focused on phytoplankton physiology of the surface layer, the future study
10 may also need to address the response of subsurface phytoplankton community to the frontal dynamics
11 over the shelf, since both the light field and nutrient conditions may vary substantially at the subsurface
12 layer across the salinity front.

13

14 **5 Conclusions**

15 Overall, the importance of physical-biological interaction in driving the patterns of phytoplankton
16 physiology and size-fractionated growths within a strong plume-induced salinity front over the NSCS
17 shelf was investigated by intense field measurements and shipboard incubation experiments during
18 April-June 2016. The current study suggested that variability of phytoplankton nutrient limitation and
19 size-fractionated growth on the shore-side, the seaside, and the frontal zone of the shelf-sea frontal
20 system could be attributed to varying nutrient supplies driven by physical dynamics of the frontal
21 system. While the impact of river plume was to directly increase the growth rates of all the three
22 phytoplankton size-classes, both nano- and pico-cells could become saturated with a high percentage of
23 plume water at the frontal zone. Vertical mixing or upwelling was found to substantially improve
24 surface phytoplankton growth over both sides of the front by altering the nutrient concentrations and
25 ratios. These results are important for a better understanding of physical control of coastal ecosystem
26 dynamics in the NSCS shelf-sea.

27



1 Acknowledgements

2 We thank the captain and the staffs of *R/V Zhanjiang Kediao* for helps during the cruises. Drs Jie Xu
3 and Dongxiao Wang were acknowledged for cruise assistants. This work is supported by the National
4 Key Research and Development Program of China (2016YFC0301202) and the National Natural
5 Science Foundation of China (41676108, 41706181).

6

7 Reference

8 Acha, E.M., Mianzan, H.W., Cuerrero, R.A., Favero, M., and Bava, J.: Marine fronts at the continental
9 shelves of austral South America: Physical and ecological processes, *J. Mar. Syst.*, 44, 83-105,
10 2004.

11 Alexander, H., Rouco, M., Haley, S.T., et al.: Functional group-specific traits drive phytoplankton
12 dynamics in the oligotrophic ocean, *PNAS*, 112, 5972–5979.

13 Cai, W., Dai, M., Wang, Y., et al.: The biogeochemistry of inorganic carbon and nutrients in the Pearl
14 River estuary and the adjacent Northern South China Sea, *Cont. Shelf Res.*, 24(12), 1301-1319,
15 2004.

16 Cermeño P, Marañón, E., Rodríguez, J., et al.: Large-sized phytoplankton sustain higher carbon specific
17 photosynthesis than smaller cells in a coastal eutrophic ecosystem, *Mar. Ecol. Prog. Ser.*, 297,
18 51-60, 2005.

19 Chen Y.L.L., Chen, H.Y., Karl, D.M., and Takahashi, M.: Nitrogen modulates phytoplankton growth in
20 spring in the South China Sea, *Cont. Shelf Res.*, 24, 527-541, 2004.

21 Cui, D., Wang, J., and Tan, L.: Response of phytoplankton community structure and size-fractionated
22 chlorophyll-a in an upwelling simulation experiment in the western South China Sea . *J. Ocean*
23 *Univ. China*, 15(5), 835-840, 2016.

24 Dagg, M.J., Benner, R., Lohrenz, S.E., and Lawrence, D.: Transformation of dissolved and particulate
25 materials on continental shelves influenced by large rivers: plume processes, *Cont. Shelf Res.*, 24,
26 833-858, 2004.

27 Dong, L., Su, J., Wong, L., Cao, Z., and Chen J.: Seasonal variation and dynamics of the Pearl River



1 plume, *Cont. Shelf Res.*, 24(16), 1761–1777, 2004.

2 Finkel, Z.V., Beardall, J., Flynn, K.J., Quigg, A., Rees, T.A.V., and John A. Raven, J.A.: Phytoplankton
3 in a changing world: cell size and elemental stoichiometry, *J. Plankton Res.*, 32(1), 119–137, 2010.

4 Franks, P.J.S.: Phytoplankton blooms at fronts: patterns, scales, and physical forcing mechanisms, *Rev.*
5 *Aqua. Sci.*, 6, 121-131, 1992.

6 Fong, D.A., and Geyer, W.R.: Response of a river plume during an upwelling favorable wind event, *J.*
7 *Geophys. Res.*, 106(C1), 1067-1084, 2001.

8 Gan, J., Cheung, A., Guo, X., and Li, L.: Intensified upwelling over a widened shelf in the northeastern
9 South China Sea, *J. Geophys. Res.*, 114, C09019, doi: 10.1029/2007JC004660, 2009.

10 Gan, J., Lu, Z., Cheung, A., Dai, M., Liang, L., Harrison, P.J., and Zhao X.: Assessing ecosystem
11 response to phosphorus and nitrogen limitation in the Pearl River plume using the Regional Ocean
12 Modeling System (ROMS), *J. Geophys. Res.*, 119(12), 8858-8877, doi:10.1002/2014JC009951,
13 2014.

14 Garvine, R.W., and Monk, J.D.: Frontal structure of a river plume, *J. Geophys. Res.*, 79(15), 2251-2259,
15 1974.

16 Harrison, P.J., Yin, K., Lee, J.H.W., Gan, J., and Liu, H.: Physical-biological coupling in the Pearl
17 River Estuary, *Cont. Shelf Res.*, 28, 1405-1415, 2008.

18 Horner-Devine, A.R., Hetland, R.D., and Macdonald, D.G.: Mixing and transport in coastal river
19 plumes, *Ann. Rev. Fluid Mech.*, 47(47), 569-594, 2015.

20 Knap, A., Michaels, A., Close, A., Ducklow, H., Dickson A.: Protocols for the Joint Global Ocean Flux
21 Study (JGOFS) Core Measurements, JGOFS Report No 19, 170pp, 1996.

22 Li, Q. P., Franks, P.J.S., Ohman, M.D., and Landry, M.R.: Enhanced nitrate fluxes and biological
23 processes at a frontal zone in the Southern California current system, *J. Plankton Res.*, 34, 790–801,
24 2012.

25 Li Q. P., Dong, Y., and Wang, Y.: Phytoplankton dynamics driven by vertical nutrient fluxes during the
26 spring inter-monsoon period in the northeastern South China Sea, *Biogeosci.*, 13, 1–12, 2016.

27 Litchman E, Klausmeier, C.A., Schofield, O.M., and Falkowski, P.G.: The role of functional traits and
28 trade-offs in structuring phytoplankton communities: scaling from cellular to ecosystem level, *Ecol.*



1 Lett., 10, 1170–1181, 2007.

2 Liu, K., Chao, S., Shaw, P., Gong, G., Chen, C., and Tang, T.: Monsoon-forced chlorophyll distribution
3 and primary production in the South China Sea: observations and a numerical study, Deep-Sea Res.
4 I, 49, 1387–1412, 2002.

5 St. Laurent, L.: Turbulent dissipation on the margins of the South China Sea, Geophys. Res. Lett., 35,
6 L23615, doi:10.1029/2008GL035520, 2008.

7 Lohrenz, S.E., Redalje, D., Cai, W., Acker J., and Dagg, M.: A retrospective analysis of nutrients and
8 phytoplankton productivity in the Mississippi River Plume, Cont. Shelf Res., 28(12), 1466-1475,
9 2008.

10 Marañón, E.: Cell size as a key determinant of phytoplankton metabolism and community structure,
11 Ann. Rev. Mar. Sci., 7, 241–264, 2015

12 Marañón, E., Cermeño, P., Latasa, M., and Tad, R.D.: Temperature, resources, and phytoplankton size
13 structure in the ocean, Limnol. Oceanogr., 57, 1266-1278, 2012.

14 Marañón, E., Cermeño, P., Latasa, M., and Tad, R.D.: Resource supply alone explains the variability of
15 marine phytoplankton size structure, Limnol. Oceanogr., 60, 1848–1854, 2015.

16 McAndrew, P.M., Bjorkman, K.M., Church, M.J., et al.: Metabolic response of oligotrophic plankto
17 communities to deep water nutrient enrichment, Mar. Ecol. Prog. Ser., 332, 63-75, 2007.

18 Moore, C.M., Mills, M.M., Arrigo, K.R., et al.: Processes and patterns of oceanic nutrient limitation,
19 Nat. Geosci., 6(9), 701-710, 2013.

20 Morgan, C.A., Robertis, A.D., and Zabel, R.W.: Columbia River plume fronts. I. Hydrography,
21 zooplankton distribution, and community composition, Mar. Ecol. Prog. Ser., 299, 19-31, 2005.

22 Ou, S., Zhang, H., and Wang, D.: Horizontal characteristics of buoyant plume off the Pearl River
23 Estuary during summer, J. Coast Res., 50, 652-657, 2007.

24 Raven, J.A.: The twelfth Transley Lecture. Small is beautiful: The picophytoplankton, Func. Ecol., 12,
25 503–513, 1998.

26 Su, J.: Overview of the South China Sea circulation and its influence on the coastal physical
27 oceanography outside the Pearl River Estuary, Cont. Shelf Res., 24, 1745–1760, 2004.

28 Suttle CA, Cochlan, W.P., and Stockner, J.G.: Size-dependent ammonium and phosphate uptake, and



1 N:P supply ratios in an Oligotrophic Lake, *Can. J. Fish. & Aqua. Sci.*, 48(48), 1226-1234, 1991.

2 Wong, L.A., Chen, J.C., Xue, H., Dong, L., Guan, W., and Su, J.: A model study of the circulation in
3 the Pearl River Estuary and its adjacent coastal waters: 2 Sensitivity experiments, *J. Geophys. Res.*,
4 108(C5), 249–260, 2003.

5 Wong, G. T., Tseng, C., Wen, L., Chung, S.: Nutrient dynamics and N-anomaly at the SEATS station,
6 Deep-Sea Res. II, 54(54), 1528-1545, 2007.

7 Wu, J., Chung, S., Wen, L., Liu, K., Chen, Y.L., Chen, H., and Karl, D.M.: Dissolved inorganic
8 phosphorus, dissolved iron, and Trichodesmium in the oligotrophic South China Sea, *Global
9 Biogeochem. Cycle*, 17(1), 1008–1016, 2003.

10 Yin, K., Qian, P., Wu, M., Chen, J., Huang, L., Song, X., and Jian W.: Shift from P to N limitation of
11 phytoplankton biomass across the Pearl River estuarine plume during summer, *Mar. Ecol. Prog. Ser.*, 221: 17-28, 2001.

13 Zhang, J., Yu, Z., Wang, J., Ren, J., Chen, H., Xiong, H., Dong, L., and Xu, W.: The subtropical
14 Zhujiang (Pearl River) Estuary: nutrient, trace species and their relationship to photosynthesis,
15 *Estuar. Coast. Shelf Sci.*, 49(3), 385–400, 1999.

16



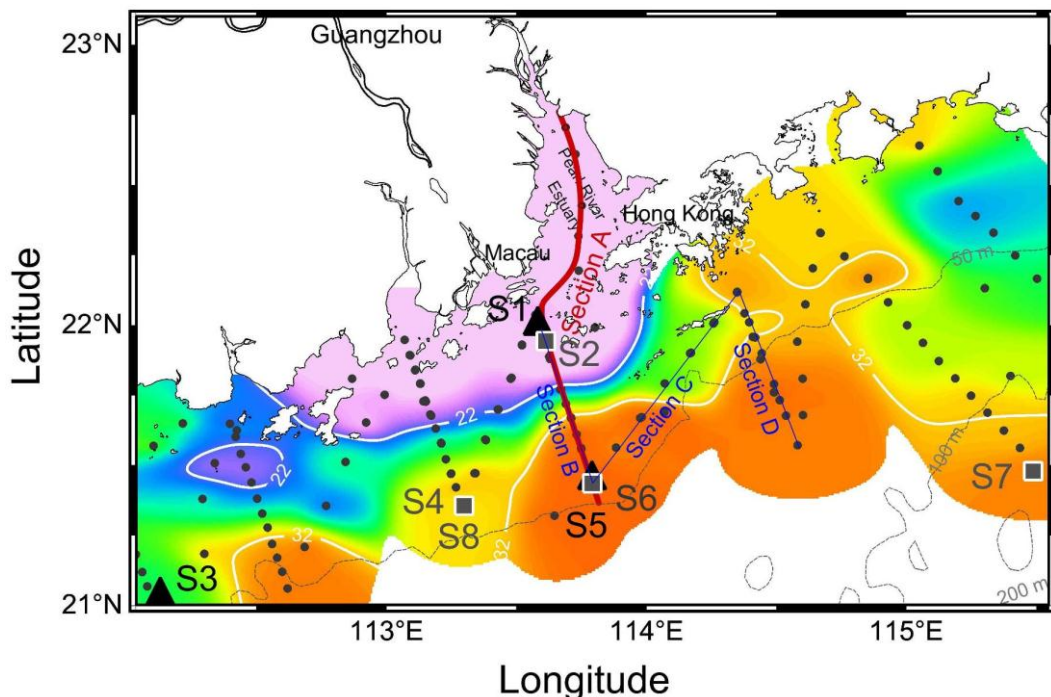
1 **Table 1.** Hydrographic and biogeochemical properties of the surface and bottom waters for incubations
 2 over the NSCS shelf during May and June 2016.

Stati on	Date	Depth [m]*	T [°C]	S [%]	Chl- <i>a</i> [μ g L ⁻¹]	micro [%]	nano [%]	pico [%]	Si [μ M]	N+N [μ M]	SRP [μ M]	N/P
S1	5/18	1	24.5	20.4	7.01	73.8	14.3	11.9	34.1	33.3	0.22	151
		10	23.6	31.7	7.93	37.4	5.6	56.9	16.4	20.1	0.32	63
S2	6/19	1	29.1	6.6	6.82	19.9	65.8	14.2	192.5	45.4	0.83	55
		8	25.6	34.0	0.31	12.1	65.3	22.5	43.9	16.7	0.65	28
S3	5/15	1	27.9	30.9	0.91	35.3	39.2	25.5	3.2	16.6	0.13	127
		50	20.9	34.5	0.34	17.9	43.2	38.9	4.3	7.7	0.22	35
S4	6/18	1	30.0	30.7	1.24	5.5	43.8	50.7	1.2	6.6	0.21	32
		39	21.7	34.6	0.91	4.9	32.6	62.5	10.8	6.1	0.23	26
S5	5/19	1	26.6	34.4	0.26	1.3	8.8	89.9	1.4	1.0	0.09	12
		36	23.8	34.3	0.15	15.0	27.9	57.1	2.0	1.3	0.11	11
S6	6/19	1	30.7	34.5	0.73	0.3	23.8	75.8	2.2	0.5	0.14	3
		47	21.7	34.7	0.45	9.2	21.0	69.8	9.3	3.6	0.17	21
S7	6/21	1	30.8	32.1	0.59	0.7	45.1	54.2	1.3	3.3	0.07	46
		109	19.2	34.7	0.07	1.4	11.0	87.6	13.3	9.2	0.61	15

3 *The depth of surface water is always at ~1 m with the depth of bottom water 5-10 m above the topography.



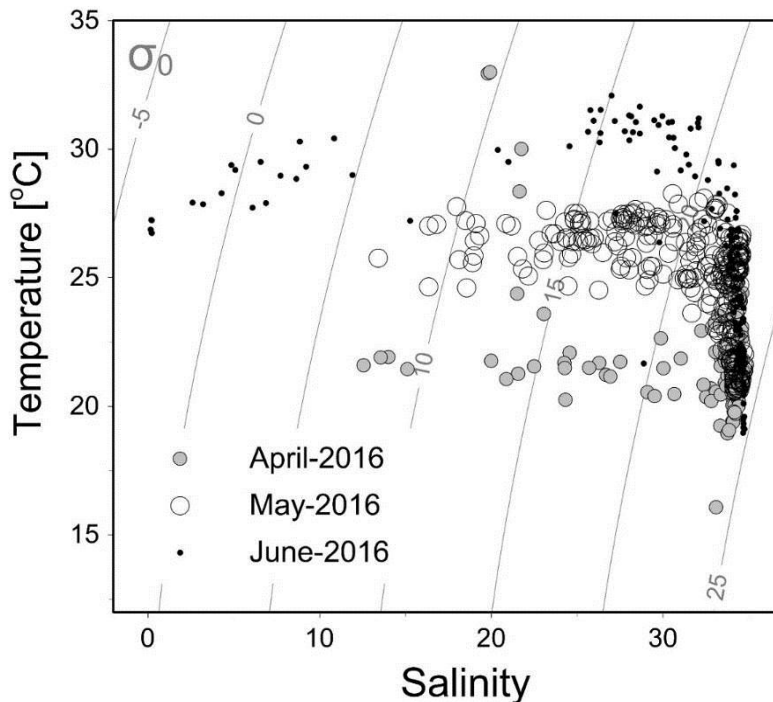
1



2

3

4 **Figure 1.** Sampling map in the NSCS shelf during May-June 2016. Color is the surface salinity with the
5 frontal zone by white lines of 26 and 32 (nearshore and offshore boundaries of the plume); Section A
6 across the front from the PRE to the shelf; section B across the front with sections C and D on the
7 seaside; triangles and squares are incubation sites S1-S7; dots are the stations with dash lines the
8 isobaths.



1
2
3
4
5

Figure 2. A Temperature vs. Salinity diagram during May-June 2016. Filled circles, open circles, and dots are data of April, May and June cruises, respectively.

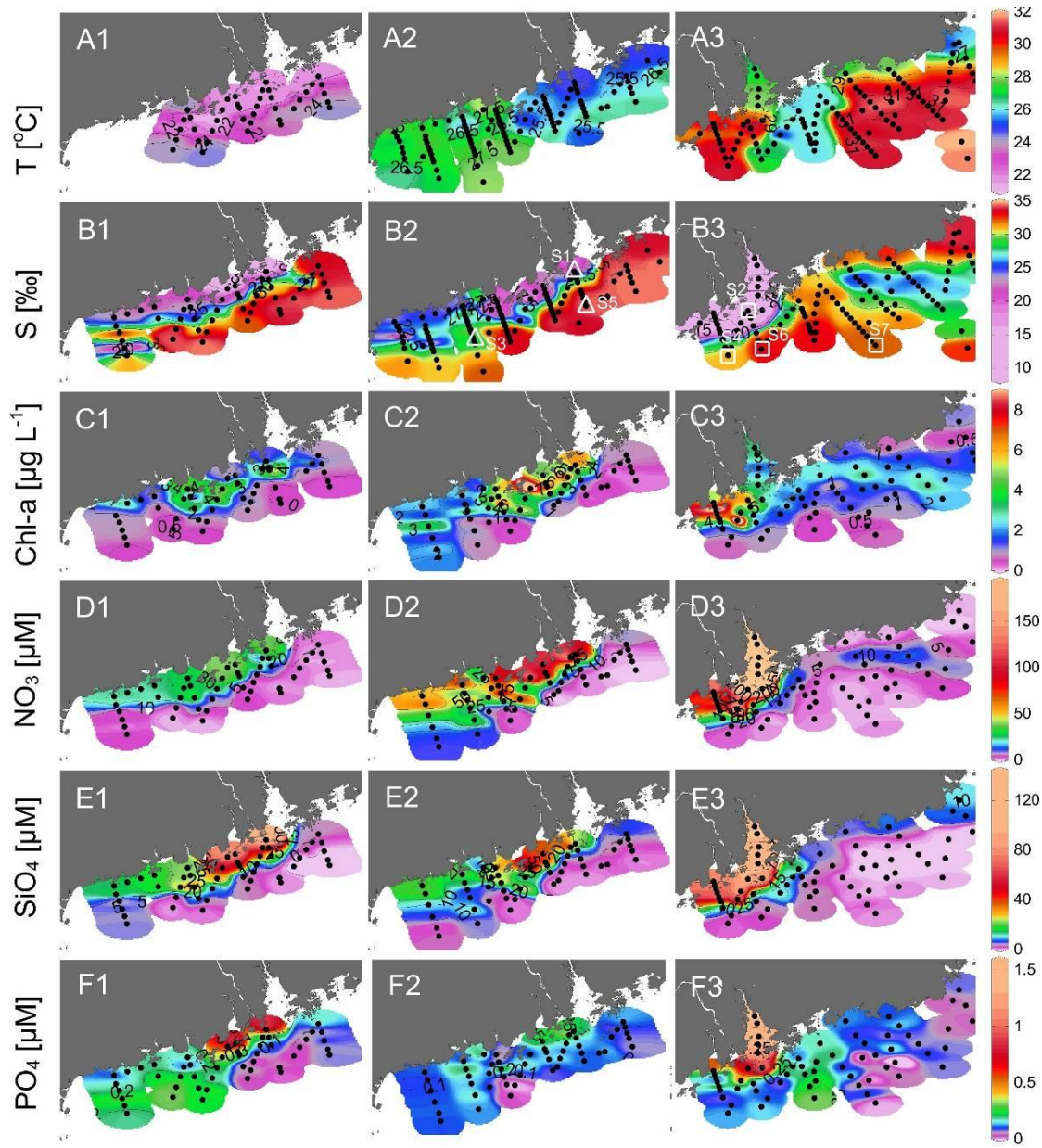


Figure 3. Surface distributions of (A1-A3) temperature, (B1-B3) salinity, (C1-C3) chlorophyll-*a*, (D1-D3) nitrate, (E1-E3) silicate, and (F1-F3) phosphate in the NSCS during April, May, and June 2016. Small dots are the data points; open triangles and squares in B2-B3 show the positions of S1-S7.

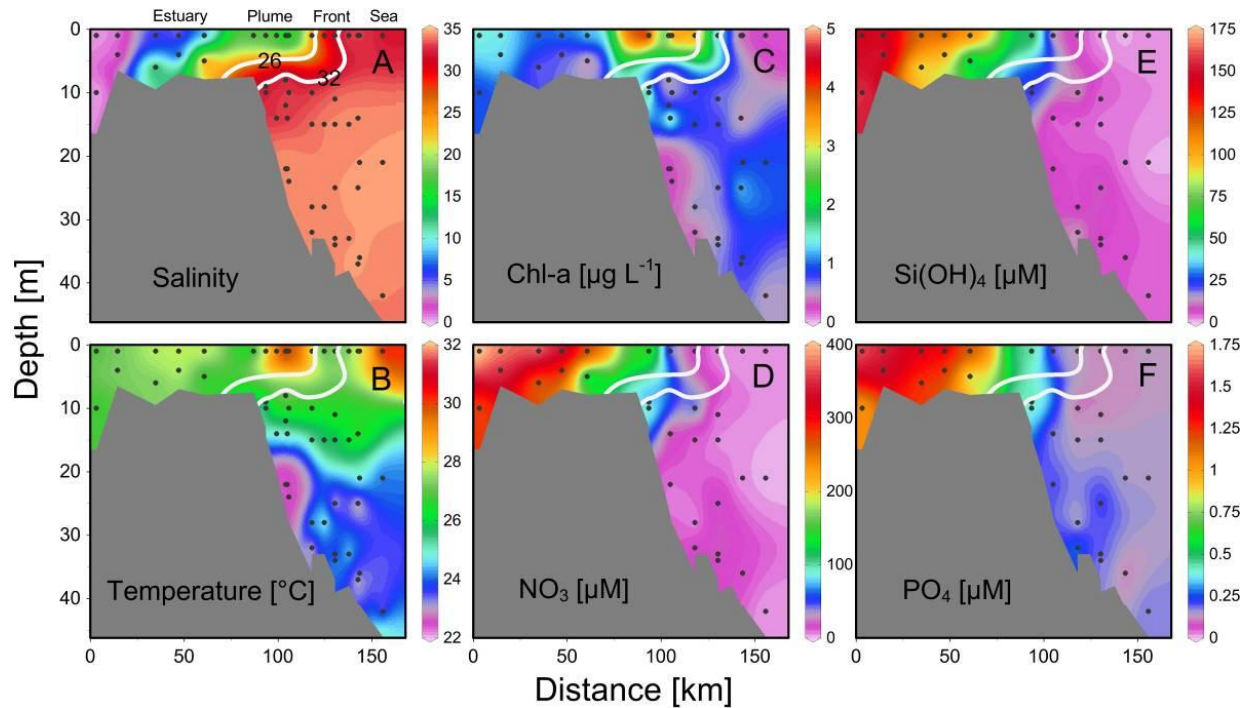
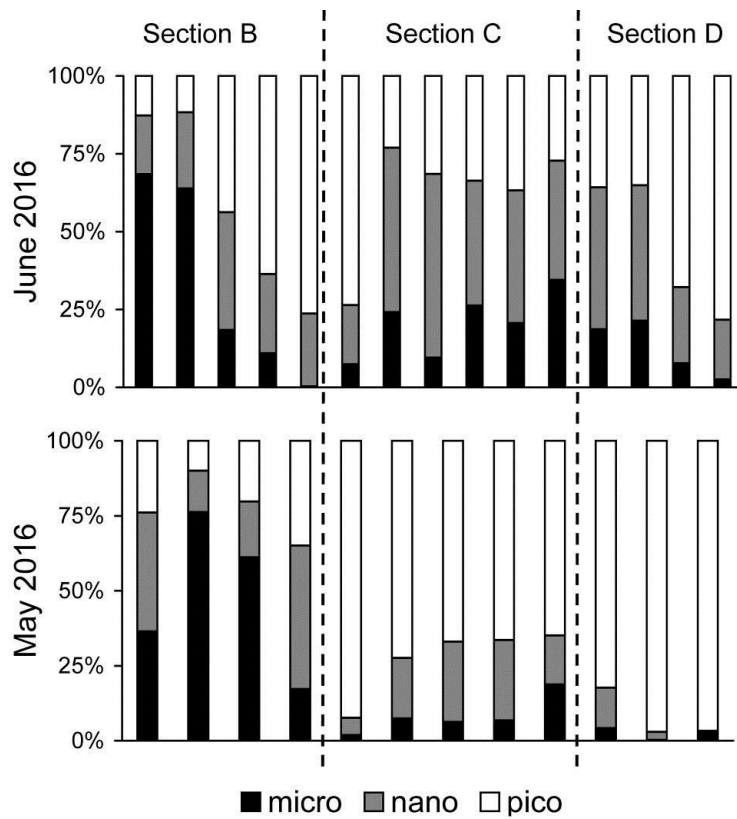


Figure 4. Vertical distribution of (A) salinity, (B) temperature, (C) chlorophyll-*a*, and (D) nitrate, (E) silicate, and (F) phosphate across the front from the estuary to the sea. Location of the section is in Fig.1. Two white lines overlaid are salinity of 26 and 32 for nearshore and offshore boundaries of the plume (see text for detail).

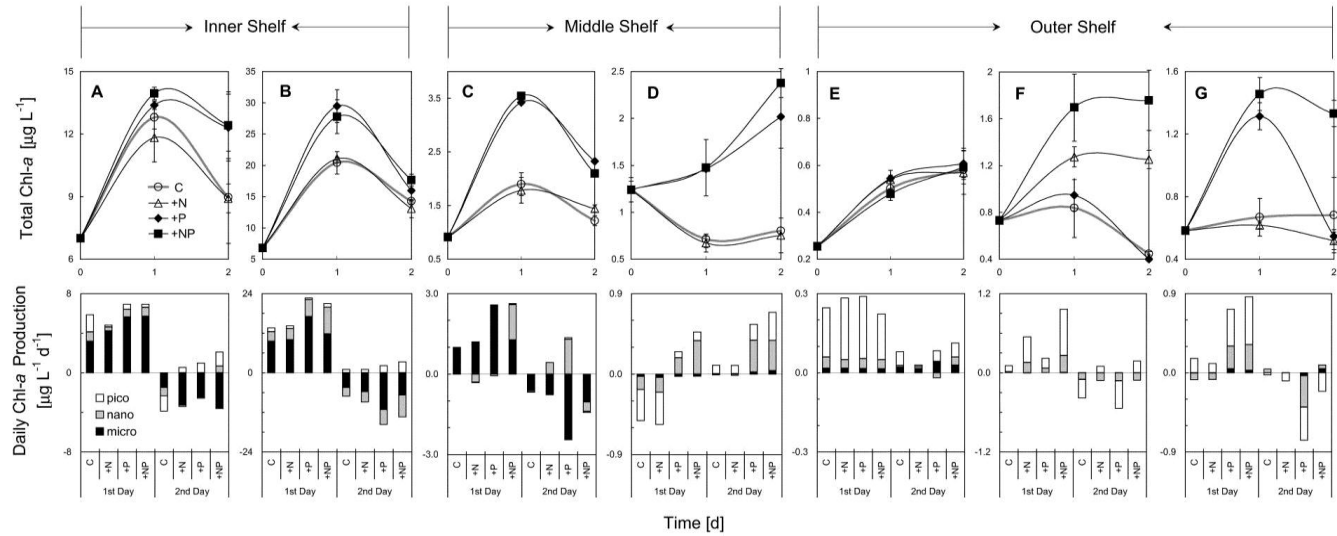


1

2

3 **Figure 5.** Comparisons of size-fractionation chlorophyll-*a* for sections B, C, and D between May and
4 June 2016.

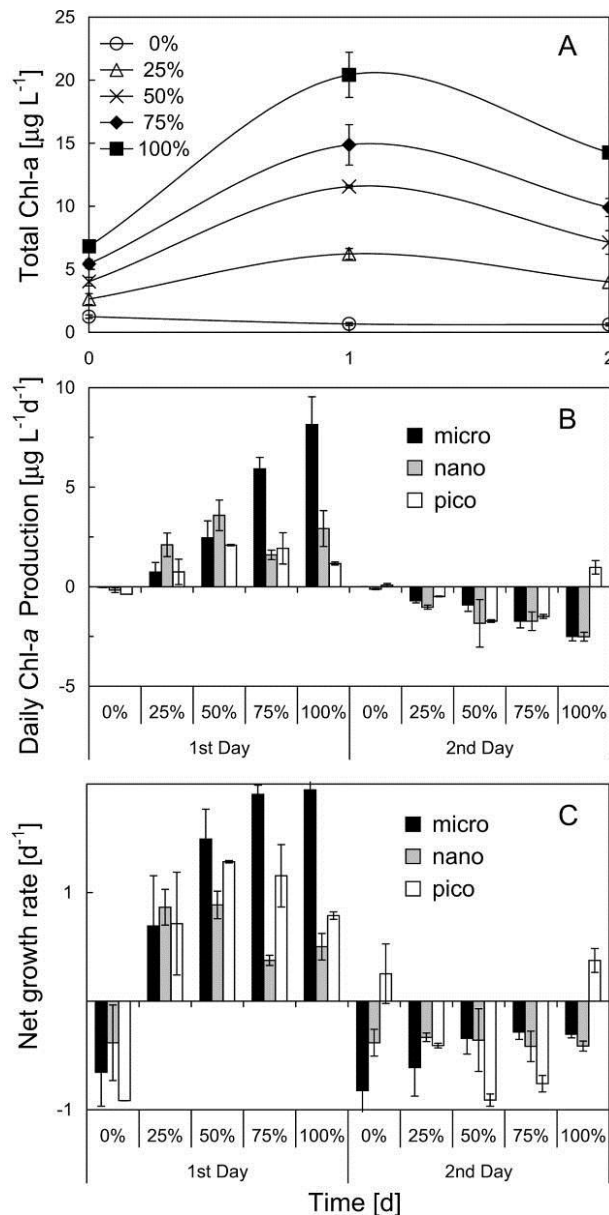
5



1

2

3 **Figure 6.** Responses of total chlorophyll-*a* and size-fractionated daily chlorophyll-*a* production rate of
4 the surface water to various nutrient enrichments at (A) S1, (B) S2, (C) S3, (D) S4, (E) S5, (F) S6, and
5 (G) S7 during May and June 2016. Station locations are in Figure 1 with the initial conditions in Table
6 1; Treatments include control (C), nitrogen alone (+N), phosphorus alone (+P), and nitrogen plus
7 phosphorus (+NP), respectively.



1
2
3 **Figure 7.** Responses of (A) total chlorophyll-*a*, (B) size-fractionated rate of daily chlorophyll-*a*
4 production, and (C) size-fractionated net growth rate of the surface water at S4 to a various percentage
5 of plume water from S2.
6

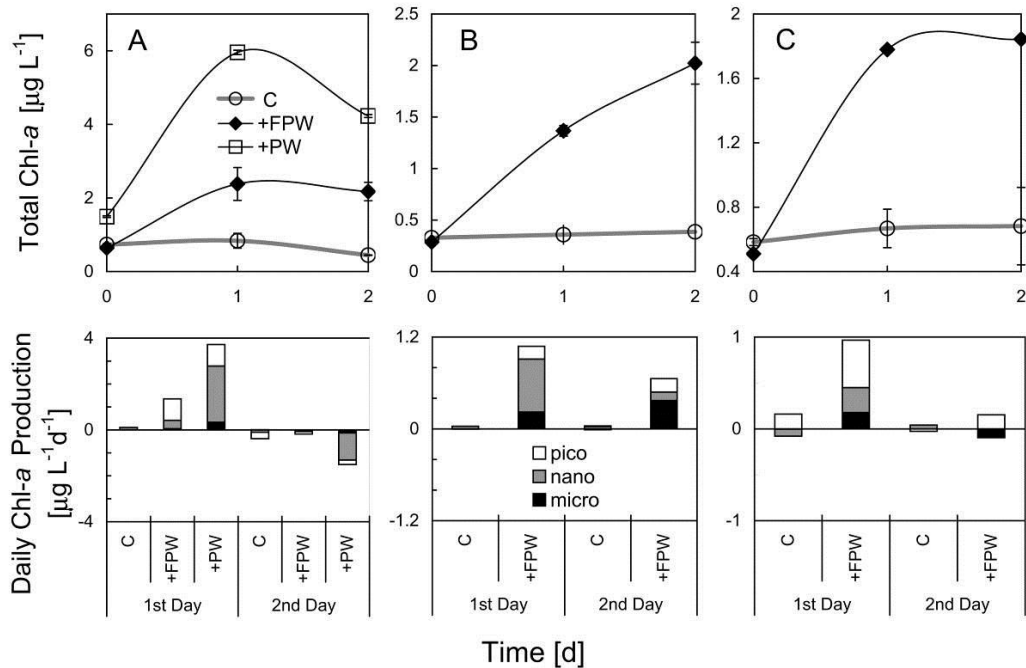


Figure 8. Responses of total chlorophyll-*a* and size-fractionated rate of daily chlorophyll-*a* production of the surface water to the addition of plume water at (A) S6, (B) S7, and (C) S8. PW is the plume water with FPW the filtered plume water.

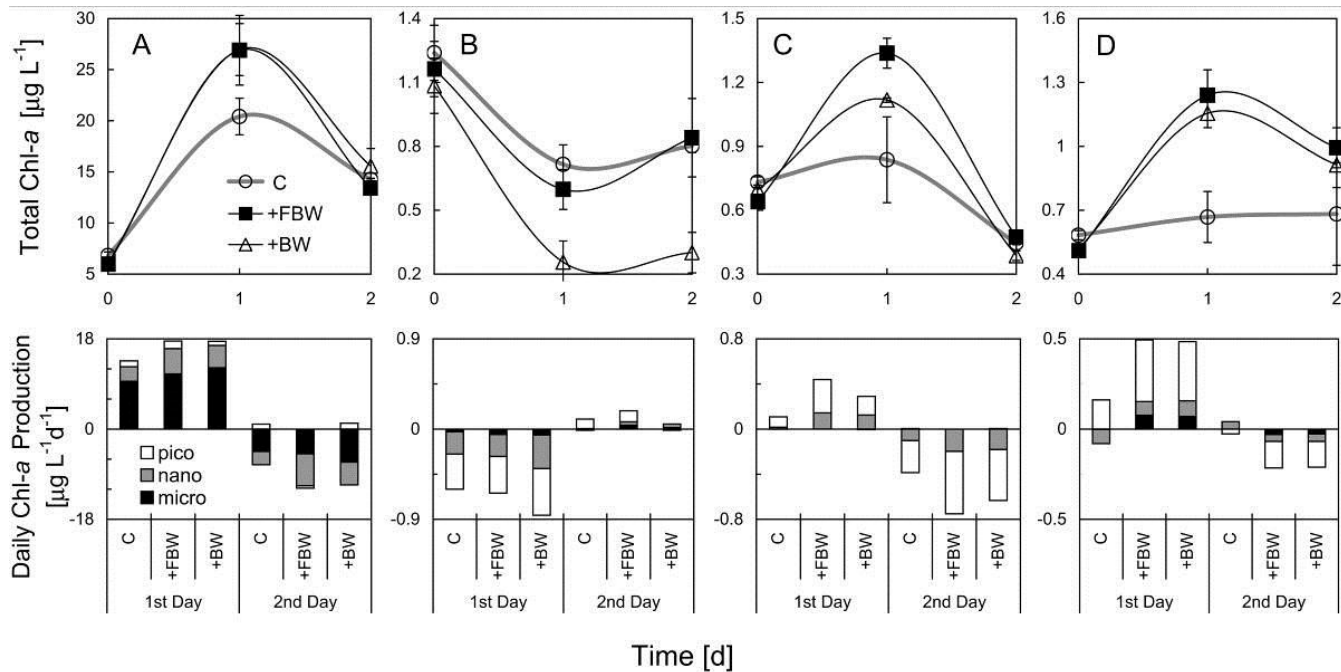


Figure 9. Responses of total chlorophyll-*a* and size-fractionated rate of daily chlorophyll-*a* production of the surface water to the addition of local bottom waters at station **(A)** S2, **(B)** S4, **(C)** S6, and **(D)** S7 during June 2016. BW is the bottom water with FBW the filtered bottom water.